Foundation Analysis, Preliminary Investigation

H. McGinness and M. S. Katow
DSN Engineering Section

The known solution of a semi-infinite plate with normal forces on its edge is compared to the computed results of an assembly of solid finite elements in Nastran.

I. Introduction

The azimuth bearing of large antennas is usually an annular runner for hydrostatic support pads or a circular track for support wheels. In either case the foundation for the bearing is a cylindrical concrete pedestal or footing which supports the whole weight of the antenna. During construction, the runner or track is positioned accurately a few centimeters above the foundation, and then the intervening space is packed with grout or other suitable stable substance. It is desirable to have good estimations for both the deflection of the bearing and for the maximum compressive stress in the supporting grout. Rigorous analyses of these quantities have been difficult in the past. Current general-purpose structural analysis programs, such as Nastran, have the capability of modeling the problem with an assembly of finite element plates.

In an attempt to ascertain the fineness of the grid point spacing required to give acceptable results, a relatively simple problem was modeled which has a known closed form solution. By comparing the results of a few models of different fineness to the exact solution, the fineness required to produce satisfactory results can be determined because this problem is intimately related to the real azimuth bearing configuration.

II. The Related Simple Problem

The relatively simple problem is the determination of the deflection and stresses in a semi-infinite plate having a uniformly distributed pressure applied over a finite length of its edge. Since the pads or wheel groups of the real bearing are spaced far apart on a large radius, it is believed that the semi-infinite plate approximates the real problem insofar as vertical deflections are concerned. A discussion of the maximum grout stresses when a runner or track is interposed between the applied load and grout will appear in a subsequent report.

In Fig. 1 is shown the pressure loading p on the semi-infinite plate. The origins of the spacial coordinates Y and R are the edge of the undeflected plate and the center of the loaded area, respectively. The vertical deflections V of the edge of the plate parallel to coordinate Y are derived by a coordinate transformation of the equations of Ref. 1, page 92, and are as follows:

$$V_c = \frac{2ap}{\pi E}[(1-\nu) + 2\ln\zeta - (1-\lambda)\ln(1-\lambda) - (1+\lambda)\ln(1+\lambda)], \quad \lambda \leq 1 \tag{1}$$

$$V_0 = \frac{2ap}{\pi E}[(1-\nu) + 2\ln\zeta + (\lambda-1)\ln(\lambda-1) - (\lambda+1)\ln(\lambda+1)], \quad \lambda \geq 1 \tag{2}$$

where

V_c is the surface deflection under the loaded area of length $2a$

V_0 is the surface deflection outside the loaded area

p is the applied uniform pressure load

E is the modulus of elasticity of the semi-infinite plate

ν is Poisson's ratio

$\zeta = d/a$ where d is the vertical distance beneath the center of the loaded area at which the deflection is assumed to be zero

$\lambda = R/a$, where R is the horizontal coordinate

Equations (1) and (2) may be evaluated conveniently over a large range of λ by the following single equation:

$$V = \frac{2ap}{\pi E}[(1-\nu) + 2\ln\zeta + f(\lambda)] \tag{3}$$

where the value of $f(\lambda)$ is given by the curve of Fig. 2. This curve represents the relative deflections of points on the edge of the plate.

The first and second derivatives of the vertical displacements are as follows:

$$\frac{dV_c}{dR} = \frac{2p}{\pi E}[\ln(1-\lambda) - \ln(1+\lambda)], \quad \lambda < 1 \tag{4}$$

$$\frac{d^2V_c}{dR^2} = \frac{2p}{\pi aE}\left[\frac{-2}{1-\lambda^2}\right], \quad \lambda < 1 \tag{5}$$

$$\frac{dV_0}{dR} = \frac{2p}{\pi E}[\ln(\lambda-1) - \ln(\lambda+1)], \quad \lambda > 1 \tag{6}$$

$$\frac{d^2V_0}{dR^2} = \frac{2p}{\pi aE}\left[\frac{2}{\lambda^2-1}\right], \quad \lambda > 1 \tag{7}$$

The horizontal displacements at the surface are:

$$U_c = -\frac{(1-\nu)}{E}pR, \quad R \leq a \tag{8}$$

$$U_0 = -\frac{(1-\nu)}{E}pa, \quad R \geq a \tag{9}$$

The principal stresses are derived from Ref. 1, pages 89–92. Figure 3 defines the two principal directions, namely, radial and tangential. The principal stresses at any point P are:

$$\sigma_{radial} = \frac{-p}{\pi}(\alpha + \sin\alpha) \tag{10}$$

$$\sigma_{tangential} = \frac{-p}{\pi}(\alpha - \sin\alpha) \tag{11}$$

For points a distance d beneath the center of the loaded area, the radial (vertical) principal stress is

$$\sigma_{radial} = \frac{-p}{\pi}\left[2\arctan\frac{a}{d} + \sin\left(2\arctan\frac{a}{d}\right)\right] \tag{12}$$

III. Finite Element Model

The finite element model was built up of solid hexahedron isoparametric elements, each element having 12 straight edges and eight corners attached to grid points. A one-element-thick layered model, as shown in Fig. 4, was built up using a simple computing program to generate all of the necessary input data.

Symmetric plane constraints were generated for the centerline and one side of the plane of elements to simulate a plate. Ground constraints were attached to the bottom nodes (points of zero vertical deflections). An alternate solution used additional side constraints to simulate a two-dimensional problem.

Two mesh patterns were used. The finer mesh configuration used the finest mesh size E equal to $a/4$. As the distance increased from the load point and the centerline, the element size for one dimension was increased along both the horizontal and vertical direction; that is, the

aspect ratio increased. The coarse mesh configuration started with E equal to $a/2$.

The computed results are presented in dimensionless units. For the Y deflection along the top surface in Fig. 5, the constant in Eq. (3) was transposed and $V\pi E/2ap$ was plotted against the horizontal distance R/a. The exact solution using Eq. (3) is shown as the solid line, and the fine mesh model answers with one-sided constraints are shown by the dotted line.

Compressive stresses on the vertical centerline are compared in Fig. 6. The exact solution for stress calculation uses a model infinitely deep while the finite element model has a fixed depth of 14.5a. The stresses at the center of the hexahedron elements are compared to the exact solution on the centerline for the same depth.

IV. Conclusions

1. The vertical deflections comparison along the horizontal line using the one-sided constraints in the finite element model shows an adequate match for practical use. With the alternate two-dimensional constraint use, the match was closer. Our second thoughts are that the alternate model is a closer simulation to the exact model, as the stresses are constant throughout the cross section for this model.

2. The compressive stress comparisons using the computed center stresses in the isoparametric hexahedron element show a good match of the results even though the finite element model must be cut off at a definite depth. The coarse mesh model has adequate accuracy.

Reference

1. Timoshenko, *Theory of Elasticity*, 1st ed., p. 92, McGraw-Hill, New York, 1934.

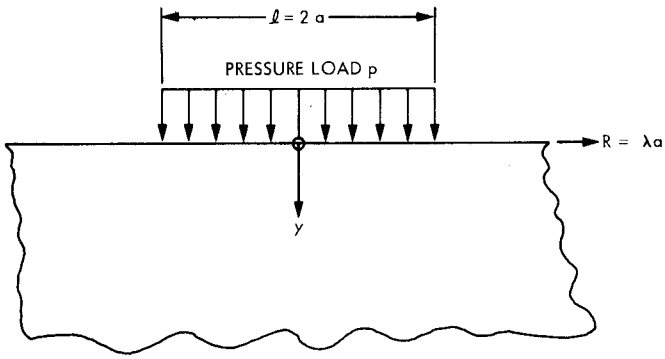

Fig. 1. Configuration of loading on semi-infinite plate

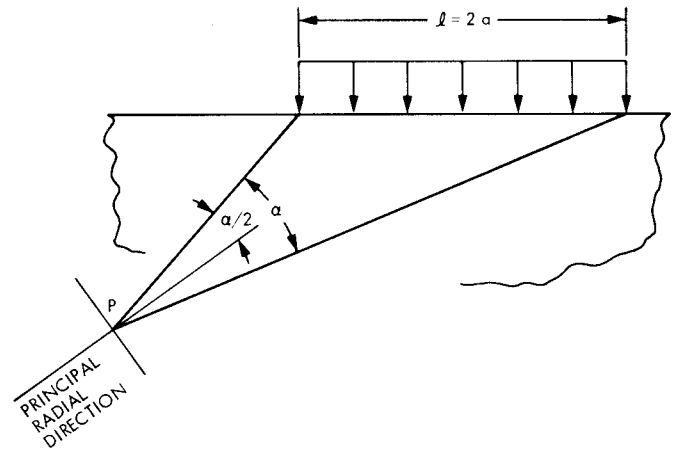

Fig. 3. Principal stress directions

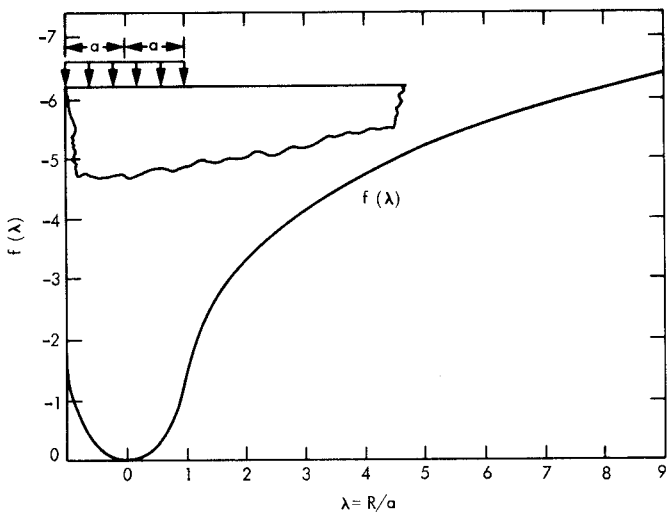

Fig. 2. Relative deflections of points on edge of plate

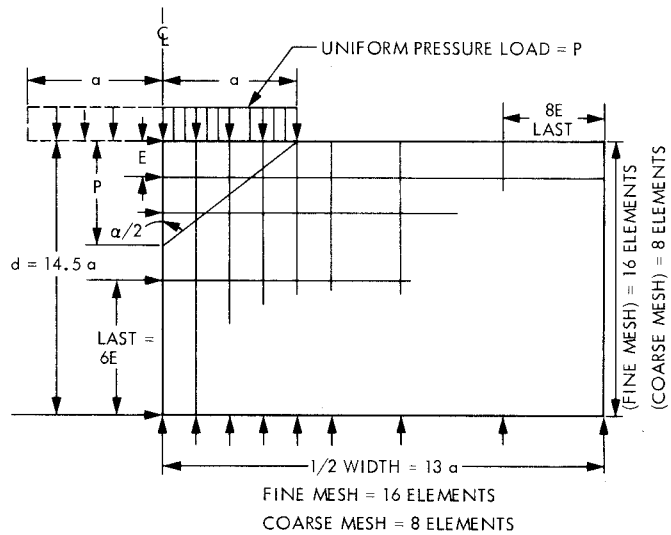

Fig. 4. Configuration of finite elements

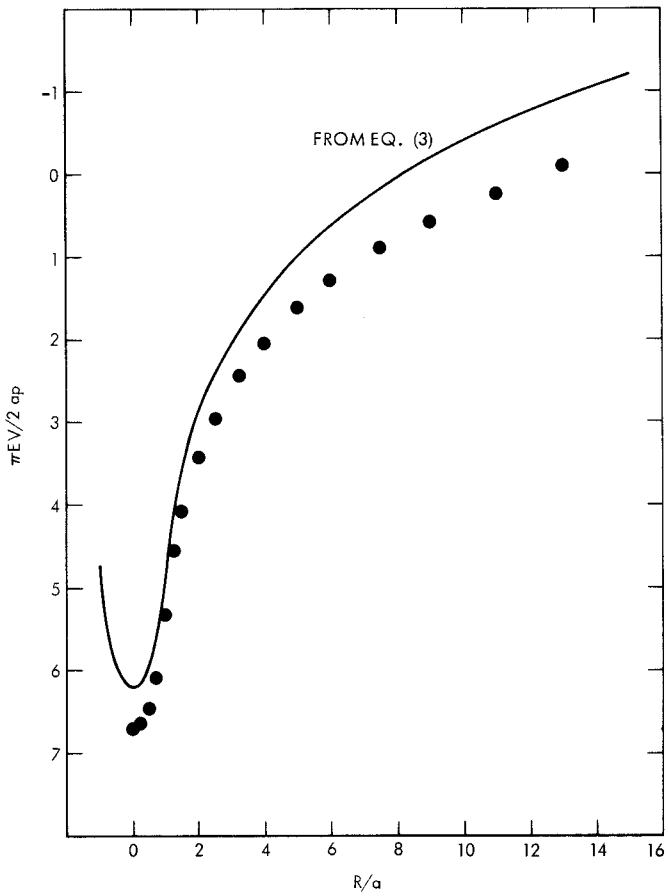

Fig. 5. Vertical deflections vs horizontal distance

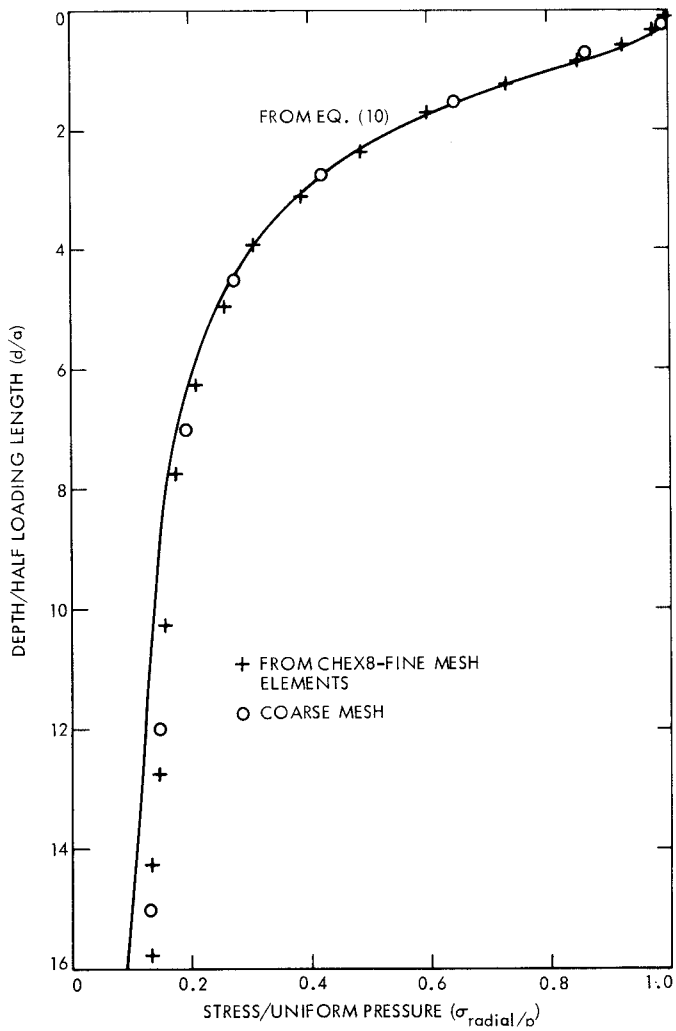

Fig. 6. Compressive stress at the vertical centerline